Available online at www.sciencedirect.com
SCIENCE DIRECT®
Solid State Nuclear Magnetic Resonance 29 (2006) 183–190
Solid State Nuclear Magnetic Resonance
www.elsevier.com/locate/ssnmr

Solid-state NMR structural studies of the fibril form of a mutant mouse prion peptide $PrP_{89–143}$(P101L)

Kwang Hun Lim[a], Tuan N. Nguyen[a,b], Steven M. Damo[a,b], Tanya Mazur[a,c], Haydn L. Ball[d], Stanley B. Prusiner[d], Alexander Pines[a,c], David E. Wemmer[a,b,*]

[a]*Department of Chemistry, University of California, USA*
[b]*Lawrence Berkeley National Laboratory, Physical Biosciences, Berkeley, CA 94720-1460, USA*
[c]*Material Science Divisions, Lawrence Berkeley National Laboratory, Berkeley, CA 94720-1460, USA*
[d]*Institute for Neurological Disease, University of California, San Francisco, CA 94143, USA*

Received 30 June 2005; received in revised form 7 September 2005
Available online 26 October 2005

Abstract

The peptide fragment 89–143 of the prion protein (carrying a P101L mutation) is biologically active in transgenic mice when in a fibrillar form. Injection of these fibrils into transgenic mice (expressing full length PrP with the P101L mutation) induces a neurodegenerative prion disease (Kaneko et al., J. Mol. Biol. 295 (2000) 997). Here we present solid-state NMR studies of $PrP_{89–143}$(P101L) fibrils, probing the conformation of residues in the hydrophobic segment 112–124 with chemical shifts. The conformations of glycine residues were analyzed using doubly $^{13}C=O$ labeled peptides by two-dimensional (2D) double-quantum correlation, and double-quantum filtered dephasing distance measurements. MQ-NMR experiments were carried out to probe the relative alignment of the individual peptides fibrils. These NMR studies indicate that the 112–124 segment adopts an extended β-sheet conformation, though not in a parallel, in register alignment. There is evidence for conformational variability at Gly 113. DQ correlation experiments provide useful information in regions with conformational heterogeneity.

Keywords: Prion; Solid-state NMR; Double-quantum NMR; Multiple-quantum NMR; Alignment; β-helix

1. Introduction

The accumulation of protein aggregates in the human body is believed to underlie a significant number of diseases [1–4]. These include transmissible spongiform encephalopathies (prion diseases Creutzfeld Jacob disease (CJD), bovine spongiform encephalopathy (BSE), etc.), type II diabetes, Alzheimer's and Parkinson's diseases. At least 16 different proteins or polypeptides have been associated with these "amyloid" diseases [1]. A common feature of amyloid diseases is the conversion of soluble, often globular proteins to fibrillar forms that are insoluble aggregates. There is increasing evidence that early soluble aggregates rather than fibrils are the species toxic to cells [2], but all of the proteins involved do also form fibrillar aggregates. Spectroscopic and fiber diffraction data indicate that peptides in these fibrils are predominantly in β-sheet conformations arranged such that the backbones of β-strands run perpendicular to the fibril axis (termed cross-β structure)[5]. Various biophysical studies have shown that fibrils formed from different peptides have common structural properties, being straight and unbranched with diameters of 40–120 Å, although there is no similarity in amino acid sequence or native structure of the various amyloid forming proteins.

Knowing the detailed structure of different peptides in these amyloid fibrils is of importance in investigating the

Abbreviations: PrP, prion protein; MQ, muliple quantum; DQ, double quantum; CJD, Creutzfeld Jacob disease; BSE, bovine spongiform encephalopathy; Aβ, amyloid beta peptide; DRAWS, dipolar recoupling with a windowless sequence; CPMG, Carr–Purcell–Meiboom–Gill; EM, electron microscopy

*Corresponding author. Fax: 510 486 6059.
E-mail address: dewemmer@lbl.gov (D.E. Wemmer).

0926-2040/$ - see front matter © 2005 Elsevier Inc. All rights reserved.
doi:10.1016/j.ssnmr.2005.09.017

mechanism of amyloid formation, and thus numerous structural studies of fibrils have been carried out. However, fibrils are insoluble, non-crystalline materials to which X-ray crystallography and solution state NMR cannot be applied. A variety of solid-state NMR techniques have been developed and applied to amyloid fibrils, and have successfully addressed some of the fundamental issues [6–10]. For example, multiple quantum (MQ) experiments [11] have been used to determine the relative alignments of the individual β-strands to be parallel or not, evidence for each has been found for different peptides in fibrils. Regions of non-β-strand conformations have also been identified [12]. Recently, a detailed structural model for the amyloid beta peptide (Aβ)-amyloid (1–40) fibril was proposed based on extensive solid-state NMR studies [13]. In this model the 40 residue peptides have the first 10 residues disordered, residues 12–24 and 30–40 as β-strands, and connecting residues 25–29 forming a turn. The resulting 'hairpin' peptides are hydrogen bonded and associate along the fibril axis with individual peptide 'hairpins' running parallel to each other. To understand what features of peptides in fibrils are general it is important to compare this structure of Aβ with those formed by peptides from different amyloidogenic proteins.

Prion diseases are different from other amyloid diseases in that pathogenic (also called scrapie or PrP^{Sc}) forms of the prion protein (PrP) can transmit the disease from one animal to another [14]. Many efforts have been made to identify crucial residues of the protein involved in conformational conversion and infectivity. Mature PrP in cells is found as a 209 amino acid protein after processing removes signal sequences. It was shown that the *N*-terminal 'octa-repeat' region (implicated in copper binding and perhaps native function of PrP) could be proteolytically removed from the pathogenic forms without affecting infectivity [15]. Mice expressing PrP starting at residue 89 have normal susceptibility to prions and the disease progression is as in wild-type mice. A further truncation from the *N*-terminus to residue 146 resulted in mice that cannot be infected, indicating that some residues in the 89–145 segment are required for the conformational change to the infectious, scrapie form [16]. A 'mini-prion' containing residues 89–140 linked to 176–231 was shown to induce the neurodegeneration characteristic of the prion diseases in transgenic mice expressing this construct. Recently, a 55 residue peptide from the mouse PrP, carrying a proline to leucine mutation at residue 101, MoPrP(89–143, P101L) which we will abbreviate PrP^{*}_{89-143}, was shown to form amyloid fibrils in vitro. This peptide induces prion disease in transgenic mice (expressing full length PrP with the P101L mutation) when the mice are inoculated with fibrils [17]. The 55 residues contained in PrP^{*}_{89-143} are thus believed to play a central role in the conformation change from normal protein to the pathogenic forms.

^{13}C CP MAS NMR experiments have already been used to investigate secondary structure of the fibrillar, pathogenic ('infectious') and randomly aggregated ('non-infectious') forms of PrP peptides [18]. It was shown that the fibrillar form has a predominantly β-sheet conformation, while a considerable population of helical conformers exists in the randomly aggregated form. In this report, more extensive solid-state NMR studies on a particularly hydrophobic segment (residues 112–124) of the PrP^{*}_{89-143} peptide in fibrils are presented. Our experiments were designed to be able to detect residues that adopt turn conformations, as are predicted in β-helical models for this segment of PrP [19,20], and which have been observed in the 40mer Aβ peptide fibrils [12]. To obtain conformational information while avoiding spectral overlap and assignment issues, isotope labels were incorporated so that two adjacent ^{13}COs, one $^{13}C_{\alpha}$, and one Ala $^{13}C_{\beta}$ label were used in each peptide, Fig. 1. The secondary structure information was derived from ^{13}C isotropic chemical shifts for the $^{13}C_{\alpha}$ and $^{13}C_{\beta}$ labels. Two-dimensional (2D) double-quantum correlation NMR, exploiting the chemical shift anisotropy (CSA) of the two adjacent CO carbons, [21] was used to probe the structure at glycines, for which chemical shift analysis alone is less reliable. Dipolar dephasing NMR experiments were also carried out to estimate distances between the CO carbons. Probing glycines was viewed as important because of their greater conformational flexibility and common role in forming turns. MQ NMR experiments [22] were also performed on Ala $^{13}C_{\beta}$ labels to probe the relative alignment of the peptide backbones. The solid-state NMR results are discussed with respect to β-helix structural models.

GQGGGTHNQWNKLSKPKTNMKHM**AGAAAAGAVVGGL**GGYMLGSAMSRPIIHFGSD

isotopic label combinations used:

peptide 1. $^{13}C_{\alpha}$ A112; $^{13}C_{\beta}$ A114; ^{13}C=O A117 and G118

peptide 2. ^{13}C=O A112 and G113; $^{13}C_{\beta}$ A117; $^{13}C_{\alpha}$ L124

peptide 3. $^{13}C_{\alpha}$ A115; $^{13}C_{\beta}$ A116; ^{13}C=O G122 and G123

Fig. 1. Sequence of PrP(89–143)P101L (residue 101 as outline). The segment 112–124 that is the focus of this work is underlined. Sites probed with specific isotope labels in this work shown in black bold letters, and sites probed in previous work shown in bold gray letters.

2. Materials and methods

2.1. Sample preparation

Peptides were synthesized using standard Fmoc chemistry on an Applied Biosystems 433A automated peptide synthesizer (0.25 mmole scale with Rink amide MBHA resin). Unlabeled, blocked Fmoc amino acids were from Novabiochem, ^{13}C labeled alanine and glycine were from Cambridge Isotope Labs. Activation and coupling steps were as described previously [17], as were cleavage and HPLC purification. Peptide identity was verified with electrospray mass spectroscopy. Preparation of β-rich, fibrillar peptide samples also followed previous protocols [17], briefly peptide in acetate buffered saline (100 mM NaCl, 20 mM NaOAc, pH 5.0) with 50% by volume acetonitrile was incubated at 4 °C for 3 weeks (ca. 5 mg peptide/ml of solution initial concentration). Fibrils which formed (verified by electron microscopy (EM) to be typical uniform, unbranched fibrils) were harvested by centrifugation and then lyophilized.

2.2. NMR spectroscopy

All NMR spectra were acquired with a Chemagnetics 3.2 mm MAS probe, on a Varian CMX Infinity 500 spectrometer. The 2D double-quantum (DQ) NMR experiment was carried out using the dipolar recoupling with a windowless sequence (DRAWS) pulse sequence [23] with 5 ms of excitation time and a spinning speed of 3.9 kHz. Radio frequency (rf) field strengths of 33 and 90 kHz were used for the ^{13}C DRAWS pulses and ^{1}H decoupling, respectively. Samples with approximately 30 mg of labeled peptide were used for the NMR experiments. A hypercomplex 40×512 data set was acquired with a spinning frequency of 3.922 kHz and zero-filled to 128×512. In all, 800–1600 transients were averaged for each t_1 increment (15–25 μs) with an acquisition delay of 2 s. The DQ dephasing experiments were done with the sequence previously described for Carr–Purcell–Meiboom–Gill (CPMG) detection of MQ transitions [24] with the insertion of a DQ evolution period during the sequence, which allows the ^{13}C signals to be dephased under the influence of the dipolar interactions. Before the dephasing sequence, DQ filtering with 2 ms excitation and conversion was incorporated to remove natural abundance signals (Fig. 4). Pi pulses were 13.6 μs, the ^{1}H decoupling field was 90 kHz, total data acquisition was ~24 h per experiment. MQ NMR experiments with a CPMG detection scheme [24] were carried out with excitation times of 14.4 ms. Thirty-two time domain signals with a phase increment of 11.25° each were collected, an acquisition delay of 2 s (2 days total acquisition time), and then were Fourier transformed. The intensity of each order of transition was determined.

2.3. Numerical calculations

DQ and dephasing NMR experimental results were analyzed with numerical simulations using the programs GAMMA [25] and SIMPSON [26]. In order to obtain optimum (ϕ,ψ) dihedral angles, the root mean square deviations (RMSD) were calculated between experimental and simulated projected spectra along the DQ dimension in the 2D DQ/SQ correlation spectra with an increment of 10° and 20° for ϕ and ψ, respectively, and normalized by the intensities of the simulated spectra:

$$\mathrm{RMSD} = \frac{\sum_{i=-3}^{3}(S \times I_i(\mathrm{ex}) - I_i(\mathrm{sim}))^2}{\sum_{j=-3}^{3} I_j(\mathrm{sim})^2},$$

where S is a scaling factor to minimize the RMSD for each calculation. The centerband and a total of six sideband intensities were used for calculation of the RMSD between data and simulation. The 2D DQ/SQ NMR spectrum depends on the dihedral angles of the second amino acid of the labeled pair, and thus the numerical calculations will provide backbone dihedral information for it only. For dephasing experiments simulations included DQ-filtering and the effects of finite pulse lengths as well as the dipolar evolution.

3. Results

Fig. 2 shows the ^{13}C CP MAS spectra of the three differently labeled P101L mouse prion peptides obtained at a spinning frequency of 3.9 kHz. The ^{13}C NMR resonances were assigned based on chemical shifts from previous NMR studies of model peptides and proteins. It is well known that the ^{13}C isotropic chemical shift is strongly

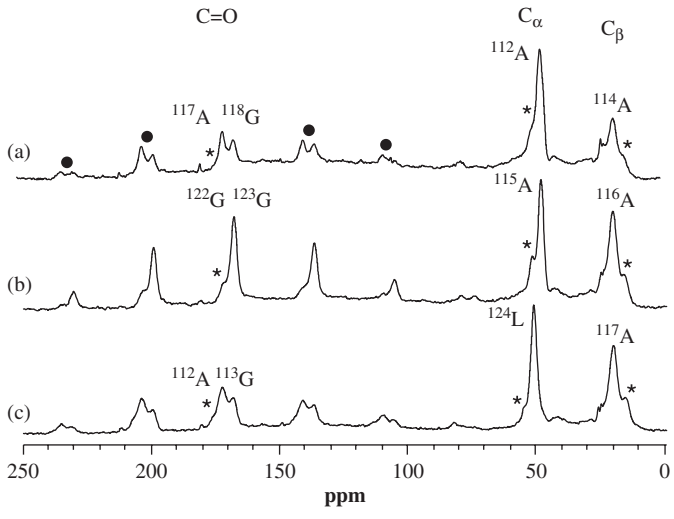

Fig. 2. ^{13}C CP MAS spectra obtained at spinning frequencies of 3.922 kHz for three prion samples ^{13}C labeled on the indicated positions and residues.A total of 400 transients were accumulated for each spectrum. The * above shoulders indicates resonances presumably from peptides that are not incorporated into fibrils. Spinning sidebands are marked with solid dots. Some weak intensity between the methyl and alpha carbon regions is likely due to natural abundance carbon from 'unlabeled' residues.

sensitive to the secondary structure [27], a property previously exploited to probe secondary structure in many peptides and proteins [28], including prion peptides [18]. Distributions of chemical shifts for different residues and conformations can be found in the BioMagResBank (www.bmrb.wisc.edu). The carbonyl resonances at ~173 and ~169 ppm are at the typical isotropic chemical shifts for Ala and Gly, respectively, in β-sheet conformations. The two Gly carbonyl resonances in Fig. 2(b) overlap at ~169 ppm. The chemical shifts of the C_α and C_β resonances from the Ala residues at ~49 and ~20 ppm also correspond to those in β-sheet conformations, if in a helix they would be expected at ~54 ppm for C_α, and ~15 ppm for C_β. The leucine C_α resonance at 53 ppm in Fig. 2(c) also corresponds to a β-sheet conformation. Small additional resonances or shoulders on peaks, marked by * in the figure, presumably come from amorphous aggregates (peptides not in fibrils taking on different conformations), as observed in our previous studies [18]; these will be discussed further below. These initial observations suggest that residues 112–124 are located in a β-strand in the fibrils.

The 2D double-quantum/single-quantum (DQ/SQ) correlation NMR experiments were carried out to further characterize the backbone structure at three glycine residues (113, 118, and 123). Fig. 3 shows the 2D DQ NMR experimental results for the three-labeled pairs containing glycine together with projections and numerical simulations of the projections. Root mean square deviations (RMSD) between the experimental and numerically calculated sideband intensities of the projected spectra, shown at the top of the 2D spectra, were calculated as a function of ϕ, and ψ dihedral angles (half the plane was sampled since spectra are invariant to a simultaneous change in sign of ϕ and ψ)· 1/RMSD was plotted in Fig. 3 to visualize optimum values more clearly. CSA values for the carbonyl carbons were determined based on the spinning sideband intensities in Fig. 2, with the assumption that the values for Gly 122 and Gly 123 are the same. For Gly 118 in Fig. 3(a), two dihedral angle ranges are found that give reasonable fits to the experimental spectra, one in the β-sheet range (−140, 130), which by visual examination of the projection agrees well, and a second with small ϕ values, (−50, −160) which is sterically disfavored even for glycine. The dipolar dephasing experiments, Fig. 4, allow us to estimate internuclear distances, and these also clearly exclude the possibility of a tight turn with small ϕ value since the predicted dipolar interaction between adjacent two carbonyl carbons (~330 Hz) would be much stronger than that from a β-strand (~180 Hz). The 1D projection, Fig. 3b, for $^{122}G^{123}G$ is quite similar to that of $^{117}A^{118}G$. The overall pattern of regions of agreement in the simulation is also similar, however the optimal fit moves to lower ϕ value, however this range is sterically not allowed. The similarity of the projection and patterns in the fits suggest that Gly 123 also adopts a β-sheet conformation. Dipolar dephasing data again support a β-sheet conformation. Together these results indicate that Gly-118 and Gly 123 are in β-strand conformations.

For the Ala-112, Gly-113 labeled peptide the lines in the 1D spectrum, Fig. 2(c), are somewhat broader than those in the other samples, though the resonances are still centered at typical β-sheet values. The 2D DQ/SQ spectrum is also weaker and substantially noisier, leading to a wider range of possible backbone angles. The dipolar dephasing and isotropic shift data are again consistent with a predominant β conformation for Gly-113. The most notable difference between the $^{112}A^{113}G$ data and $^{117}A^{118}G$ or $^{122}G^{123}G$ is in the lineshapes of the DQ/SQ data, Fig. 3 (c). For the $^{117}A^{118}G$ sample the peaks from the two-labeled residues are well separated in the SQ dimension, and both peaks give rise to a single, well-defined DQ frequency. For $^{122}G^{123}G$ the correlation is again relatively sharp, with a slight skewing of the peaks. The small downfield shifted shoulder shows a weak DQ/SQ correlation on several of the 2D peaks as a relatively sharp, distinct peak. This indicates that the frequencies of the two glycines are correlated, when one shifts downfield the other does as well. However for the $^{112}A^{113}G$ sample the frequencies are spread in both the single and DQ dimensions. The contours are strongly skewed in the direction corresponding to a slope of 2 DQ/SQ frequency (see inset in Fig. 3(c)). The spread in frequency indicates a range of chemical shifts, and the skewing indicates that the chemical shifts of the two residues change in a correlated manner [29] since the DQ dimension is the sum of the two chemical shifts of the dipolar-coupled ^{13}C spins in the SQ dimension. For completely random inhomogeneous samples, the 2D cross-peaks in the DQ/SQ correlation NMR spectrum are usually broadened in both dimensions. The peak skewing due to correlated shifts has been exploited recently to generate projected spectra with narrow lines [29]. For our PrP peptide, the lineshapes indicate that the $^{112}A^{113}G$ amino acids have a wider distribution of conformations than the other residues probed, and that their conformations are not randomly distributed as might be expected from amorphous aggregates. The most populated conformation for Gly 113 is consistent with β-sheet (strongest region in the correlation peak), extending to helical structure (lower region of the 2D contour) based on their isotropic chemical shifts. The weak centerband and two strong sideband intensities of the downfield shifted spin pairs are consistent with those of typical helical conformations [21]. Quantitative analyses of CSA values however, could not be done due to the overlap of the resonances and modest S/N ratios.

MQ NMR experiments on the alanine β carbons (methyl) of Ala-114, A-116, and Ala-117, in three different samples, and pure ^{13}C–C_β alanine as a control, were carried out to probe alignment of the β-strands in the peptide fibrils. Fig. 5 shows the experimental MQ intensities from the three peptides and pure alanine. Higher order MQ coherences, up to 8 quanta, were clearly observed with an

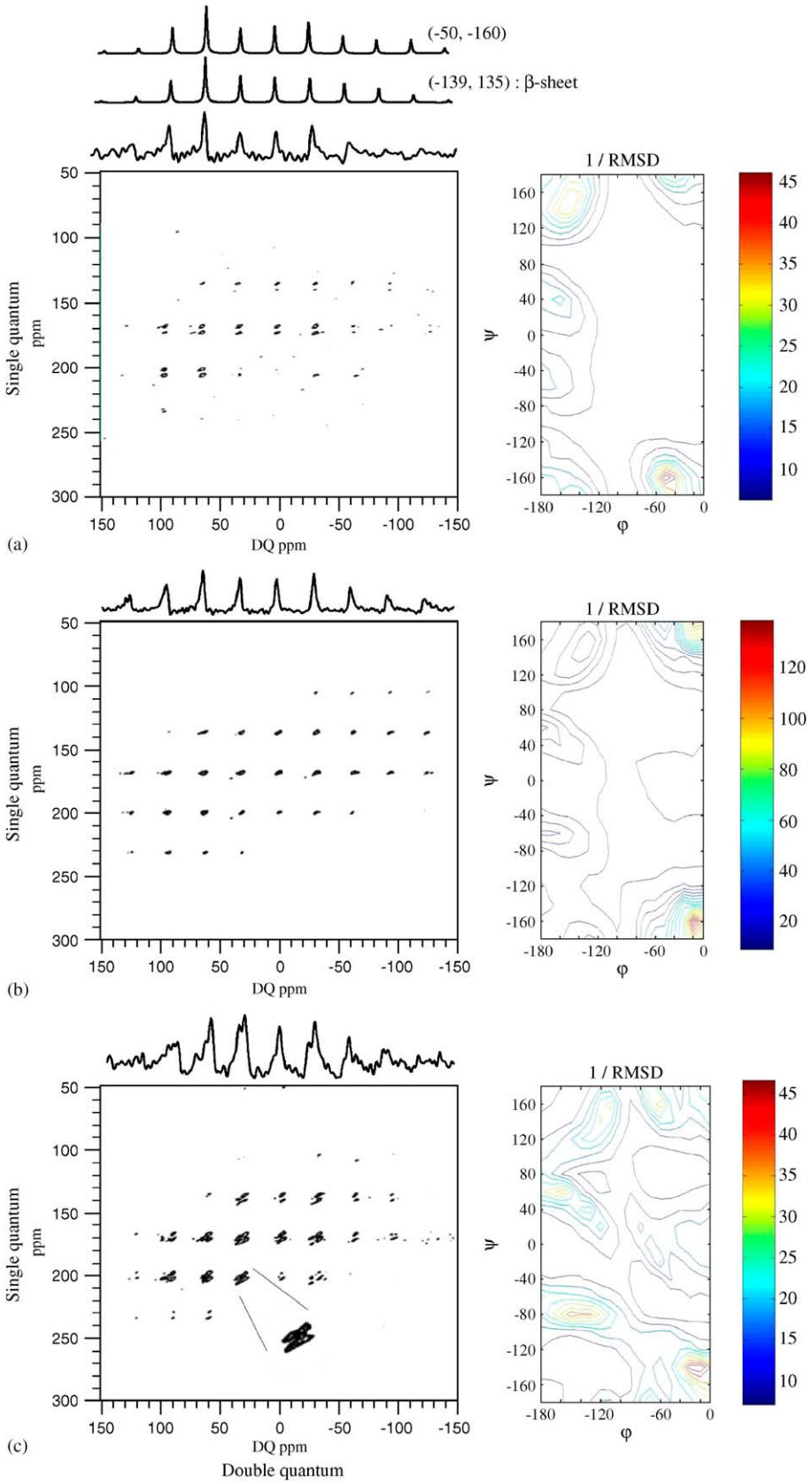

Fig. 3. Two-dimensional DQ/SQ correlation NMR spectra are shown along with a projected spectrum along the DQ dimension (top) and contour plots of the 1/RMSD as a function of dihedral angles (right) for $^{117}A^{118}G$ (a), $^{122}G^{123}G$ (b), and $^{112}A^{113}G$ (c) pairs. Calculated projection spectra (top) are shown for the $^{117}A^{118}G$ pair in (a). CSA values ($\sigma_{11}-\sigma_{iso}$, $\sigma_{22}-\sigma_{iso}$, $\sigma_{33}-\sigma_{iso}$) of (70.6, 12.6, −83.2 ppm) and (73.7, 3.2, −76.8 ppm) were used for the Alanines and Glycines, respectively, in the two AG ^{13}CO spin pairs, and (73.4, 2.8, −76.2 ppm) for the Glycines in GG spin pair in the calculations.

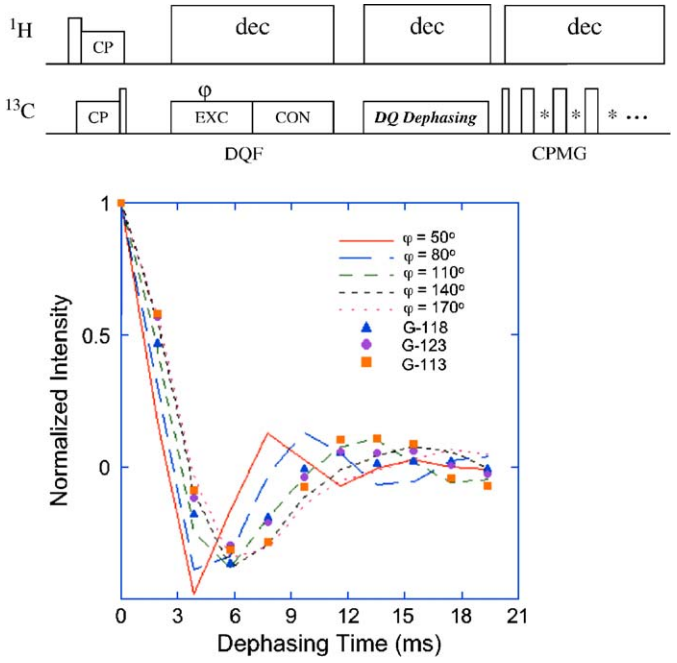

Fig. 4. Dipolar dephasing curves were generated using the pulse sequence shown at the top (CP = cross polarization; DQF = double quantum filter; DQ = double quantum dephasing; CPMG = Carr–Purcell–Meiboom–Gill echo train; dec = proton decoupling), are shown for pairs of carbonyl residues in the doubly labeled peptide samples are shown. Simulations show curves predicted for different ϕ values.

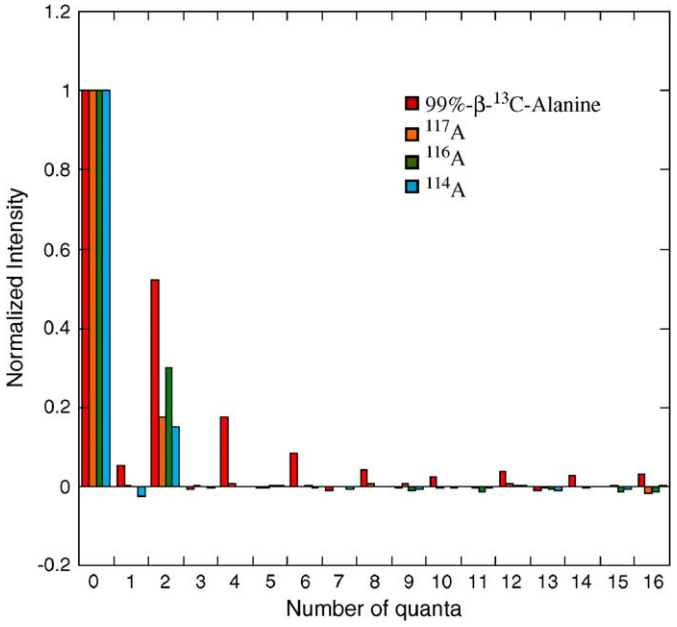

Fig. 5. Intensities of the different order MQ coherences obtained with a 14.4 ms excitation time for the 99%-3-^{13}C-Alanine in a the pure, crystalline single amino acid and in each of the three different prion peptide samples are shown.

excitation time of 14.4 ms for the pure alanine in which the minimum distance between alanine β carbons is 3.7 Å, corresponding to a dipolar coupling of 150 Hz. However, no high-order MQ coherences were detected for any of the three peptide samples with the same excitation time (14.4 ms). Although the distance between Aβ carbons in fibrils with a parallel, in register alignment is 4.8 Å (70 Hz coupling), which would result in smaller intensities of the high-order MQ coherences compared to those in pure alanine, previous numerical calculations predicted detectable amount of 4 quantum coherences, about ~10% of the 2 quantum coherence intensity at the 14.4 ms excitation time [11] as has been observed experimentally in peptides that form parallel strand sheets.

4. Discussion

Recent EM studies of 2D crystals that formed in infectious preparations of PrP isolated from brain (both $PrP^{27–30}$, and PrP^{106} with residues 141–176 deleted) were interpreted as trimeric groups of protein molecules, repeating in the 2D lattice [19]. These 2D crystals appear in preparations together with prion rods (clusters of fibrils), and may be a precursor in their formation. Previous structural models for PrP^{Sc}, or alternately a single layer β-sheet, cannot be fit well into the scattering density from the EM images. However, a β-helix model does fit the electron diffraction data well (at a resolution of ca. 10 Å), including predicted differences in scattering density between intact $PrP^{27–30}$ and PrP^{106} due to the deleted amino acids. Recent molecular dynamics (MD) calculations on Syrian hamster PrP residues 109–219 have also been found to be compatible with a structure containing a multiple strand β-sheet structure for the converted PrP, but with a completely different organization than the β-helix model for individual converted proteins in the fibrils [30]. A characteristic feature of the β-helix models is the frequent occurrence of turns, those in the left handed β-helix family (used to fit the 2D crystal data) include residues with a left-handed helical conformation (ϕ, ψ values of near +60, +60, with a wider range of ψ than ϕ), one per strand on each side of the β-helix. The MD derived model has short segments of sheet, with connecting loops. Extensive solid-state NMR studies of Aβ (1–40) fibrils have indicated that the peptides in Aβ fibrils have segments which adopt non-β-sheet conformations [12]. Given the potential importance of non-beta regions, we applied solid-state NMR experiments that could identify turns in the hydrophobic fragment 112–124, which contains a distinctive turn in the original β-helix model and a loop (112–114) in the structural model from MD calculations, of the 55 residue prion peptide fibrils. It was important to include measurements on glycines since they are frequently found in turns due to their greater conformational flexibility than other residues.

Chemical shifts from ^{13}C CP MAS experiments show that most of the residues in the 112–124 stretch are in a β-strand conformation. The 2D DQ NMR experiments also clearly indicate that Gly-118 and Gly-123 also adopt β-sheet conformations. Numerical simulations of the

experimental 2D spectra yield (ϕ, ψ) values including dihedral angles corresponding to the typical β-sheet as well as some very tight turn conformations that would be highly strained. The accuracy of the dihedral angle determination using the DQ NMR results was limited by the uncertainty of the CSA parameters, caused by the overlap of the resonances and limited S/N. Dipolar dephasing NMR experiments allow us to rule out small ϕ angle regions including tight turn conformations. Isotropic chemical shifts of the Gly CO carbons (~169 ppm) also support a β-sheet conformation [27]. The combination of experiments thus indicate that the glycines Gly-118 and Gly-123 adopt dihedral (ϕ, ψ)) angles of (-140°, 140°) and (-130°, 140°), respectively (accuracy estimated at $\pm 20^\circ$), corresponding to typical β-sheet conformations.

For Gly-113 somewhat different behavior was observed, particularly in the 2D DQ spectrum. The carbonyl resonances for the ^{112}A^{113}G pair are broader. In the 2D spectra of the ^{122}G^{123}G sample the peaks are slightly skewed, indicating a correlation in chemical shift of the two, coupled carbonyls, and there is a weak correlation from the extra peak, shifted in both dimensions. However for the ^{112}A^{113}G pair the peaks are strongly skewed, lying along a slope of ~2 DQ/SQ, indicating that chemical shifts, and hence torsional angles, of Ala-112 and G-113 are substantially correlated [29]. This indicates that the ^{112}A, ^{113}G region has more structural variability, which could reflect a region that is not as much affected by the packing within fibrils, or is in a less regular region such as a turn or loop. The C_α resonances of Ala-112 and to some extent the C_β resonance of Ala-114 also have lineshapes (Fig. 2a) suggestive of a conformational distribution in this region rather than a small amount of non-fibrillar material.

In addition to the conformation at individual residues, another important structural issue in amyloid fibrils is the relative alignment of the β-strands that are always present. Over the past few years, solid-state NMR studies have probed strand orientation in fibrils made from several different Aβ fragments with varied sequences and lengths. Fibrils formed from a small hydrophobic fragment, Aβ(34–42), adopt an antiparallel alignment [6], while parallel, in register organizations were observed for Aβ(10–35) [31] and Aβ(1–40) fibrils [11]. The register of strands relative to one another was observed to change for antiparallel Aβ(11–25) when fibrils were grown at a different pH (changing the charge distribution) [32]. Acylation of Aβ(16–22) was shown to cause a switch from antiparallel to parallel packing in amyloid fibrils [33]. In our MQ experiments of PrP^*_{89-143} peptide fibrils, no high-order MQ coherences (beyond 2Q) were detected, indicating that the 55 residue peptides do not adopt parallel, in-register β-sheet conformations. This does not, however, indicate that the fibril has an antiparallel β-sheet structure since MQ experiments will not yield the high-order MQ coherences for a distorted parallel alignment in which strands are not in register, or for a β-helix. Further NMR studies with different labeling schemes can ultimately address this issue.

The combined experimental results indicate that residues in the hydrophobic segment 112–123 of the 55 residue PrP^*_{89-143} peptide in fibrils are in extended conformations, with the residues in conformations consistent with a β-strand. Residues near 112 show variability in conformation, and hence may be located at the beginning of the ordered β-strand region that forms the core of the fibrils or in a loop or turn. We have not, to date, identified residues consistent with local right or left-handed helical conformations that are predicted for β-helix, and experimentally observed in crystal structures of β-helical proteins [34]. It is important to remember that the sequence alignments in the β-helix structures were only predicted computationally, with associated limitations in both sampling and scoring model structures. MD calculations of hamster PrP unfolding predict a different β-enriched model containing a β-sheet with three strands (residues 115–118; 128–131; 159–163, with numbering adjusted to correspond with the mouse PrP sequence), and another β-segment (residues 134–139) for the converted PrP [30]. The structure has a turn involving residues 121–123 that does not appear to be consistent with our data (we see no evidence of a turn conformation), though one should not take details of model structures too literally. Although our data are not consistent with the published β-helix model, this does not exclude the possibility that a β-helix structure exits in the 2D crystal forms of PrP^{27-30} and PrP^{106} on which the EM studies were performed [19]. We also cannot exclude the possibility that another 'register' of the sequence of PrP_{89-143} in a β-helix occurs in PrP^*_{89-143}, although a sufficient number of consecutive residues has been probed that a turn residue should have been observed if the structure has the typical 8 residues along each face of the β-helix. The turn residues are less frequent in left-handed helices, hence they also cannot be ruled out.

In the ^{13}C CP MAS spectra of all of the fibrillized peptide samples small, shifted resonances were detected for the carbonyl carbon as well as C_α and C_β signals in addition to the major peaks at typical β-sheet chemical shifts. These have been ascribed to a small amount of 'amorphous' peptide aggregates (not in fibrils, often seen in electron micrographs of fibril samples made as described here) that is conformationally more variable [18]. The amount of such material varies somewhat from sample to sample, e.g. Fig. 2(a) compared to 2(b). Because of overlap with other peaks, the presence of such material complicates the analysis of conformational distributions for peptide in the fibrils. Methods to enrich samples in fibrils would help improve the analysis. It appears that the 2D DQ/SQ correlation NMR experiments can help in characterizing NMR signals from less ordered regions in the fibril samples, and also in providing some further information about the amorphous material.

5. Conclusions

We have carried out structural studies of a biologically active, fibrillar form of the 55 residue, P101L variant prion peptide, PrP^{*}_{89-143} using solid-state NMR techniques. NMR studies focused on the hydrophobic residues from 112 to 124 to probe the backbone conformation. Analyses of the ^{13}C CP MAS, 2D double-quantum, and distance measurement NMR data indicate that residues in this part of PrP^{*}_{89-143} in fibrils mainly adopt an extended β-sheet conformation with glycine-113 in a relatively less-ordered region. The 2D DQ NMR experiment was particularly useful characterizing NMR signals from less ordered regions of peptides in fibrils, and also in distinguishing signals from random aggregates. Multiple-quantum NMR experiments using C_βs of three different alanines in fibril samples support a β-strand organization that does not have peptides parallel and in register in the prion fibrils. The data are not consistent with details of β-helix structures proposed based on electron crystallography studies [19] of Prp^{27-30} and PrP^{106} or those from recent MD calculations [30] but are not yet sufficient to rule out β-helix models in general. From measurement of PrP^{*}_{89-143} fibril diameters from electron micrographs, the full peptide would not fit if all extended β-strand indicating that there must be some turns or disordered regions, as occur in Aβ. The identification of a region of lower order at residue 112 may represent a turn or the boundary of the ordered region. Extending the labeled region is under way to distinguish these possibilities.

Acknowledgements

This work was supported in part by NIH Grant AG10770 (DEW and SBP), by the Director, Office of Science, Office of Basic Energy Sciences, Materials Science and Engineering Division, US Department of Energy under Contract No. DE-AC03-76SF00098 (AP), and by the Army Prion program, contract DMAD17-03-1-0476. SMD gratefully acknowledges an NSF pre-doctoral fellowship.

References

[1] C.M. Dobson, Philos. Trans. R. Soc. London Ser. B-Biol. Sci. 356 (2001) 133–145.
[2] M. Stefani, C.M. Dobson, J. Mol. Med. 81 (2003) 678–699.
[3] M. Sunde, C.C.F. Blake, Q. Rev. Biophys. 31 (1998) 1–39.
[4] J.C. Rochet, P.T. Lansbury, Curr. Opin. Struct. Biol. 10 (2000) 60–68.
[5] M. Sunde, L.C. Serpell, M. Bartlam, P.E. Fraser, M.B. Pepys, C.C.F. Blake, J. Mol. Biol. 273 (1997) 729–739.
[6] J.M. Griffiths, T.T. Ashburn, M. Auger, P.R. Costa, R.G. Griffin, P.T. Lansbury, J. Am. Chem. Soc. 117 (1995) 3539–3546.
[7] R. Tycko, Biochemistry 42 (2003) 3151–3159.
[8] D. Wemmer, Meth. Enzym. 309 (1999) 536–559.
[9] C.P. Jaroniec, C.E. MacPhee, N.S. Astrof, C.M. Dobson, R.G. Griffin, Proc. Natl. Acad. Sci. USA 99 (2002) 16748–16753.
[10] T.L.S. Benzinger, D.M. Gregory, T.S. Burkoth, H. Miller-Auer, D.G. Lynn, R.E. Botto, S.C. Meredith, Biochemistry 39 (2000) 3491–3499.
[11] O.N. Antzutkin, J.J. Balbach, R.D. Leapman, N.W. Rizzo, J. Reed, R. Tycko, Proc. Natl. Acad. Sci. USA 97 (2000) 13045–13050.
[12] O.N. Antzutkin, J.J. Balbach, R. Tycko, Biophys. J. 84 (2003) 3326–3335.
[13] A.T. Petkova, Y. Ishii, J.J. Balbach, O.N. Antzutkin, R.D. Leapman, F. Delaglio, R. Tycko, Proc. Natl. Acad. Sci. USA 99 (2002) 16742–16747.
[14] S.B. Prusiner, Proc. Natl. Acad. Sci. USA 95 (1998) 13363–13383.
[15] S. Supattapone, P. Bosque, T. Muramoto, H. Wille, C. Aagaard, D. Peretz, H.O.B. Nguyen, C. Heinrich, M. Torchia, J. Safar, F.E. Cohen, S.J. DeArmond, S.B. Prusiner, M. Scott, Cell 96 (1999) 869–878.
[16] T. Muramoto, M. Scott, F.E. Cohen, S.B. Prusiner, Proc. Natl. Acad. Sci. USA 93 (1996) 15457–15462.
[17] K. Kaneko, H.L. Ball, H. Wille, H. Zhang, D. Groth, M. Torchia, P. Tremblay, J. Safar, S.B. Prusiner, S.J. DeArmond, M.A. Baldwin, F.E. Cohen, J. Mol. Biol. 295 (2000) 997–1007.
[18] D.D. Laws, H.M.L. Bitter, K. Liu, H.L. Ball, K. Kaneko, H. Wille, F.E. Cohen, S.B. Prusiner, A. Pines, D.E. Wemmer, Proc. Natl. Acad. Sci. USA 98 (2001) 11686–11690.
[19] H. Wille, M.D. Michelitsch, V. Guenebaut, S. Supattapone, A. Serban, F.E. Cohen, D.A. Agard, S.B. Prusiner, Proc. Natl. Acad. Sci. USA 99 (2002) 3563–3568.
[20] C. Govaerts, H. Wille, S.B. Prusiner, F.E. Cohen, Proc. Natl. Acad. Sci. USA 101 (2004) 8342–8347.
[21] P.V. Bower, N. Oyler, M.A. Mehta, J.R. Long, P.S. Stayton, G.P. Drobny, J. Am. Chem. Soc. 121 (1999) 8373–8375.
[22] O.N. Antzutkin, R. Tycko, J. Chem. Phys. 110 (1999) 2749–2752.
[23] D.M. Gregory, D.J. Mitchell, J.A. Stringer, S. Kiihne, J.C. Shiels, J. Callahan, M.A. Mehta, G.P. Drobny, Chem. Phys. Lett. 246 (1995) 654–663.
[24] K.H. Lim, T. Nguyen, T. Mazur, D.E. Wemmer, A. Pines, J. Magn. Reson. 157 (2002) 160–162.
[25] S.A. Smith, T.O. Levante, B.H. Meier, R.R. Ernst, J. Magn. Reson. Ser. A 106A (1994) 75–105.
[26] M. Bak, J.T. Rasmussen, N.C. Nielsen, J. Magn. Reson. 147 (2000) 296–330.
[27] H. Saito, Magn. Reson. Chem. 24 (1986) 835–852.
[28] D.S. Wishart, B.D. Sykes, J. Biomolec. NMR 4 (1994) 171–180.
[29] D. Sakellariou, S.P. Brown, A. Lesage, S. Hediger, M. Bardet, C.A. Meriles, A. Pines, L. Emsley, J. Am. Chem. Soc. 125 (2003) 4376–4380.
[30] M.L. DeMarco, V. Daggett, Proc. Natl. Acad. Sci. USA 101 (2004) 2293–2298.
[31] T.L.S. Benzinger, D.M. Gregory, T.S. Burkoth, H. Miller-Auer, D.G. Lynn, R.E. Botto, S.C. Meredith, Proc. Natl. Acad. Sci. USA 95 (1998) 13407–13412.
[32] A.T. Petkova, G. Buntkowsky, F. Dyda, R.D. Leapman, W.M. Yau, R. Tycko, J. Mol. Biol. 335 (2004) 247–260.
[33] D.J. Gordon, J.J. Balbach, R. Tycko, S.C. Meredith, Biophys. J. 86 (2004) 428–434.
[34] J. Jenkins, R. Pickersquil, Prog. Biophys. Mol. Biol. 77 (2001) 111–175.